EasyChair Preprint

№ 8955

Crack Detection in Metallic Components with Varying Surface Characteristics Using Laser Spot Scanning Thermography

Sreedhar Unnikrishnakurup, Jonathan Zheng, Vinod Kumar, Carlos Manzano and Andrew Ngo

October 3, 2022

Crack detection in metallic components with varying surface characteristics using laser spot scanning thermography

Sreedhar Unnikrishnakurup [1, *], Jonathan Zheng [1], Vinod Kumar [1], Carlos Manzano[1], Andrew Ngo[1,*]

[1] *Institute of Materials Research and Engineering, 2 Fusionopolis Way, Innovis, #08-03, Singapore 138634*

**Email: sreedharun@imre.a-star.edu.sg; ngocya@imre.a-star.edu.sg*

Abstract

Cracks are the most common cause of failure in the manufacturing of metal parts, hence technologies for detecting them are essential for defect-free production. In this study, a local laser spot excitation combined with robotic scanning is used to identify vertical cracks in titanium. It is feasible to observe anisotropies in the lateral diffusivity by capturing temporal temperature data with an infrared camera utilizing local thermal stimulation. The crack parameter may then be quantified based on the regional transient behavior of temperature distribution. In doing so, we present an advanced technique for distinguishing between contrast created by the surface oxide layer and contrast caused by the vertical crack.

Keywords: Laser Thermography, Robotic scanning, surface Crack detection, NDT, FEM

1. Introduction

Infrared Thermographic (IRT) testing is an emerging field in NDE and relies on the spatio-temporally resolved detection of the heat flux within the testing object via a thermal infrared camera [1]. The heat flux is induced by an energetic source which is ideally working remotely. A very convenient and modern remote energy source is made from a high-power laser whose radiation pattern can be designed to deliver a focused spot, a line, or an area. In this way the symmetry of the induced heat flux pattern allows the testing to be optimized to different classes of defects, like, e.g., area/volume defects or linear cracks or measurement of material properties that influence the diffusion of heat. A further advantage when utilizing a laser is given by its narrow emission spectrum which is clearly separated from the infrared camera detection range. In contrast, conventional light sources like incandescent or flash lamp that are based on black body radiation often give rise to strong spurious temperature readings in the thermal detection devices. Together with high achievable power density (MW or GW per m^2) and the high repetition rate (kHz-range) laser excitation brings an unmatched flexibility into thermographic testing. The key advantage of the laser assisted infrared thermography method will be the remote nature of measurement that can hence be adapted to hostile conditions that are found in manufacturing plants.

IRT has been employed by many industries for NDE applications linked to material cracking [2] in addition to more traditional techniques including dye penetrant, magnetic particles, eddy currents and X-rays. Modeling crack thermal response for IRT applications has been the subject of several recent research [3]–[10]. The majority of thermographic crack testing research has concentrated mainly on detecting crack existence and improving the resultant crack signature. The surface characteristics of the material play an important role in the efficient measurement of cracks from the surface [11], [12]. In this work, we investigated the influence of an oxide layer on the surface of a sample and its distinguishability from crack signals during laser spot scanning thermography.

2. Materials and methods

Figure 1 depicts the schematic of the sample that was used for this study. It uses a titanium plate with 9 distinct Electrical Discharge Machined (EDM) notches, each with different aspect ratio, that measures 50.8 × 50.8 × 6.35 mm. The dimension of the notches is given Table 1. The cross-sectional view of the notch is also shown in Figure 1 Schematic of the Titanium notch sample.

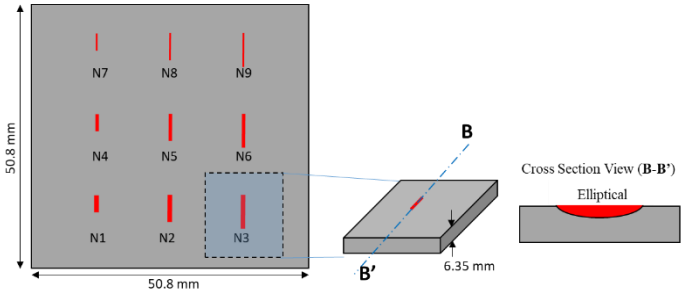

Figure 1 Schematic of the Titanium notch sample

Table 1 Dimensions of the EDM notches

Notch	**N1**	**N2**	**N3**	**N4**	**N5**	**N6**	**N7**	**N8**	**N9**
Length (mm)	0.5	0.75	1	0.5	0.75	1	0.5	0.75	1
Width (mm)	0.1	0.1	0.1	0.05	0.05	0.05	0.02	0.02	0.02
Depth (mm)	0.25	0.375	0.5	0.25	0.375	0.5	0.2	0.2	0.2

Figure 2 shows the experimental setup. The sample is placed on a sample holder and attached to the collaborative robot (cobot) to facilitate the precise scanning. A continuous wave (CW) diode laser of maximum power 22 W is used for the excitation. A Long Wave Infrared (LWIR) camera FLIR A655sc is used to capture the thermal images during the laser scanning experiment at a frame rate of 200 Hz. The sample is moved by the cobot to scan when the laser has been lit on its surface. A laser power of 3.5 W is used for the spot heating. Single linear scans were carried out using the laser spot over the same width notches at a velocity of 5 mm/s. Three different scans were realized named as N1-N2-N3, N4-N5-N6 and N7-N8-N9 scans. The name indicates the notches that covers with each scan assuming that the laser spot is passing through the center of the notches length.

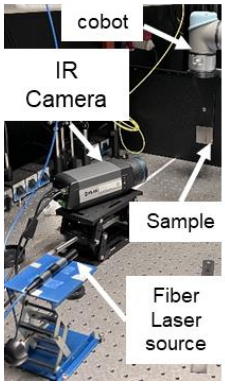

Figure 2 Experimental setup

Figure 3 depicts the different stages of a laser spot thermography scanning. The heating profile created on the surface due to the laser spot has a Gaussian distribution. When the spot scans over the surface, three-dimension diffusion phenomena take place on the surface and a unique heat distribution patterns

can be observed in a non-defective area. The three-dimensional heat diffusion is affected, and the heat flow is impeded when the laser spot approaches the crack defect zone. This blockage of heat by the crack increases the thermal resistance (R_{th}) and is shown in Figure 3. This results in the localized rise in temperature and can be identified in the captured thermographic images. When the laser spot falls directly into the laser crack area, due to the high local emissivity of the crack region, the temperature rises again, and this can be captures as a hotspot in the thermographic images. In actual samples, the surface may not have uniform emissivity, which will alter the rate of laser irradiation absorption on the sample surface and infrared thermal emission.

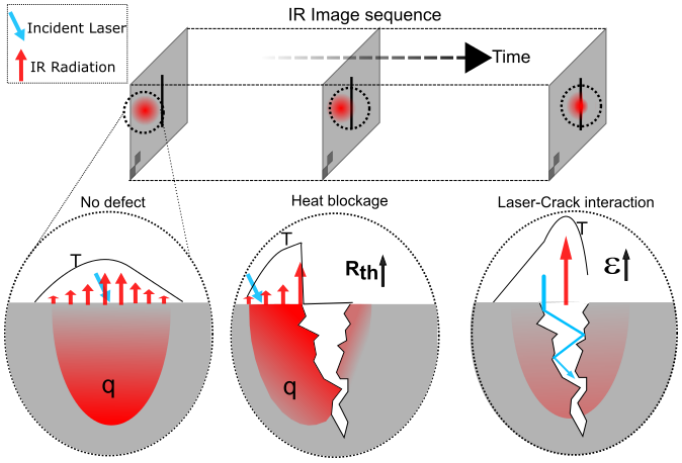

Figure 3 Defect detection mechanism using laser spot thermography

3. Results and Discussion

Figure 4 presents the experimental findings of laser spot scanning for a single scan of the sample across the notches N1, N2 and N3. The graph depicts the average temperature-time profile for nine pixels at the centre of the laser spot as the sample scans through the field of view using the cobot. The titanium sample having notches of width 0.1 mm and varying length and depth were identified as peaks in the temperature-time graph.

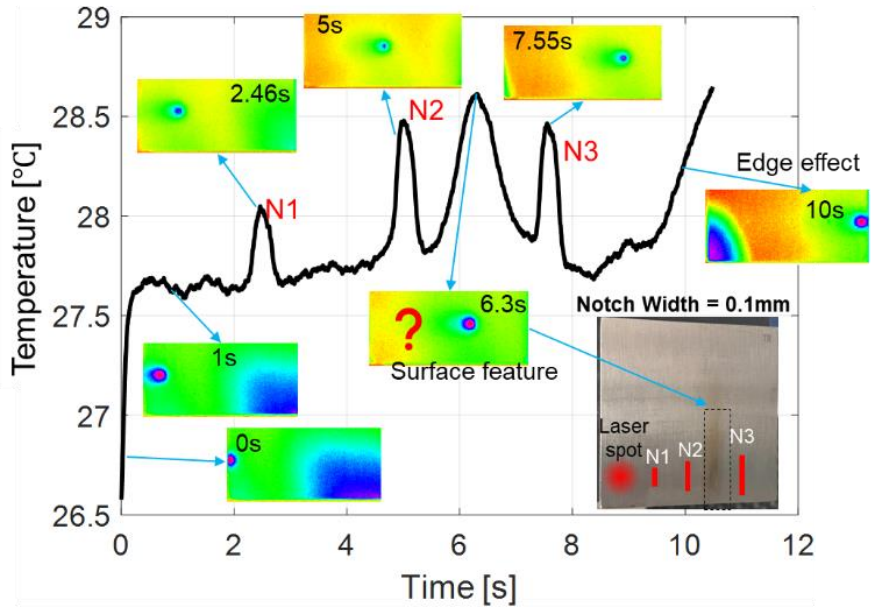

Figure 4 Point profile at laser focus for a Laser spot scanning using collaborative robot on a Titanium notch sample

As the laser spot sweeps across the sample, the thermal images corresponding to distinct time instances are also displayed on the graph. In the graph, there are five distinct peaks at time 2.46s, 5s, 6.3s, 7.55s and 10s. The photograph of the sample clearly shows that the third peak corresponds to the surface feature, as seen in Figure 4. Peak 5 corresponds to the edge effect as the laser spot approaches the edge of the sample. Peaks 1,2 and 4 have different slope features than the other two as they represent the notches. Therefore, in a real scenario inspection, the crack presence can be identified automatically using the slope representation of the temperature-time graph.

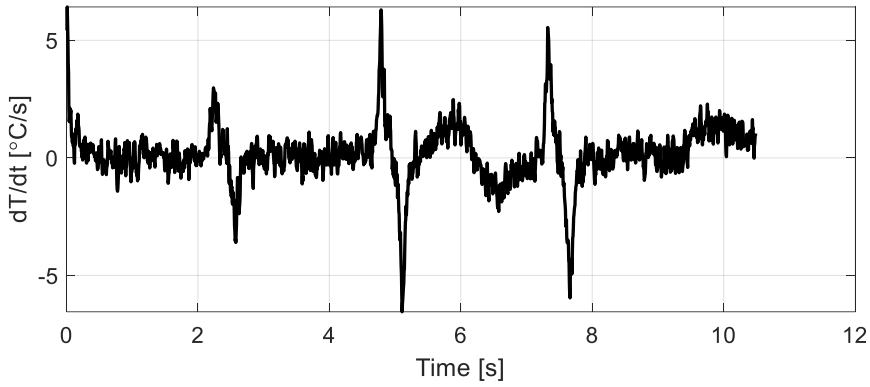

Figure 5 Derivative plots of the temperature-time graph for the bottom notch (N1-N2-N3) scan

Figure 5 shows the derivative plot (slope) of the temperature-time plot of the N1-N2-N3 scan. The derivative map clearly distinguishes between the crack peak and the peak due to the surface oxidation. When compared to the gradual slope variation caused by the surface oxidation, the sudden rise in temperature and hence the steep slope indicates the presence of crack.

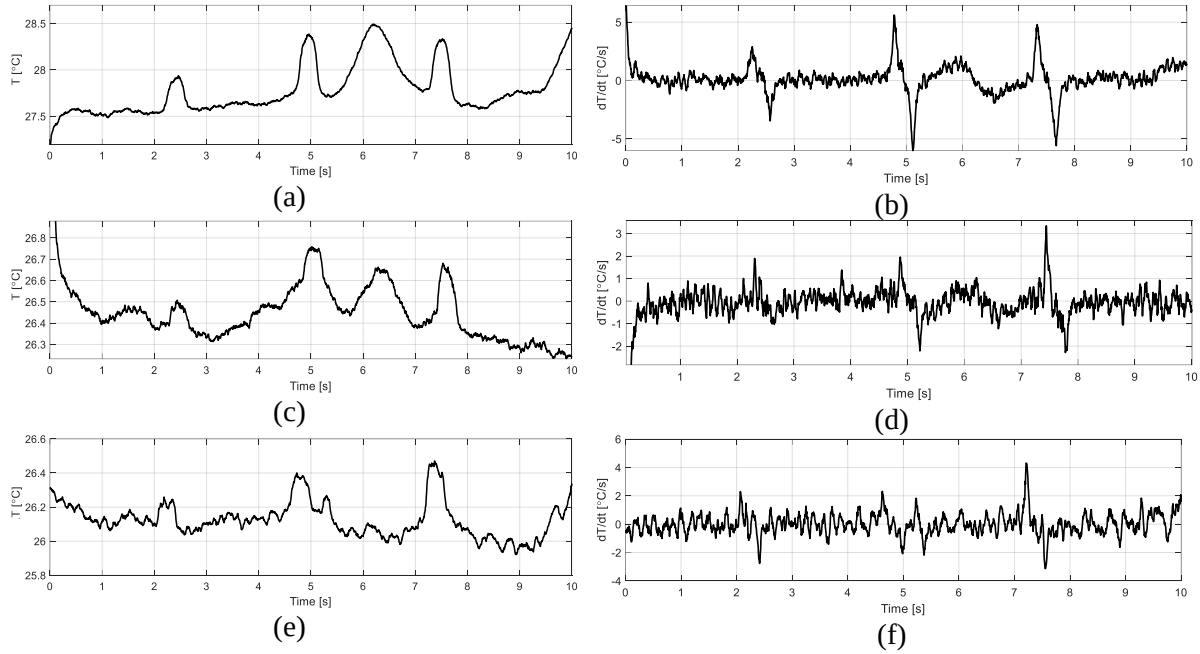

Figure 6 Temperature-time profile and Corresponding derivative plots for three different laser spot scans. (a) T-t for scan N1-N2-N3 (b) derivative(T-t) of Scan N1-N2-N3 (c) T-t for scan N4-N5-N6 (d) derivative(T-t) of Scan N4-N5-N6 (e) T-t for scan N7-N8-N9 (f) derivative(T-t) of Scan N7-N8-N9

Figure 6 presents the Temperature-time profiles and the corresponding derivative plots calculated for all the three different scans. The indication of the presence of cracks can be clearly distinguish between the presence of oxidation layer from the derivative plots. However, the crack indications signal are very minute in the case of the third scan N7-N8-N9.

Figure 7 shows the temperature map and the corresponding gradient map plotted using the temperature-time profile and the corresponding derivative plots for all the three scans. Figure 7 (a) and (b) corresponds to the scan N1-N2-N3 and the high intensity region represented by the cyan color is the path travelled by the laser spot. The laser spot is concentrated on the middle region of the crack and the crack indications therefore show a high intensity variation. However, in both other scans, the intensity of the laser spot is not placed in the center of the crack, as illustrated in Figure 7 (c) and (e), where the strength of the laser spot is positioned somewhat off from the crack center area. Nevertheless, the derivative plots were still able to capture the crack indications clearly as shown in Figure 7 (d) and (f).

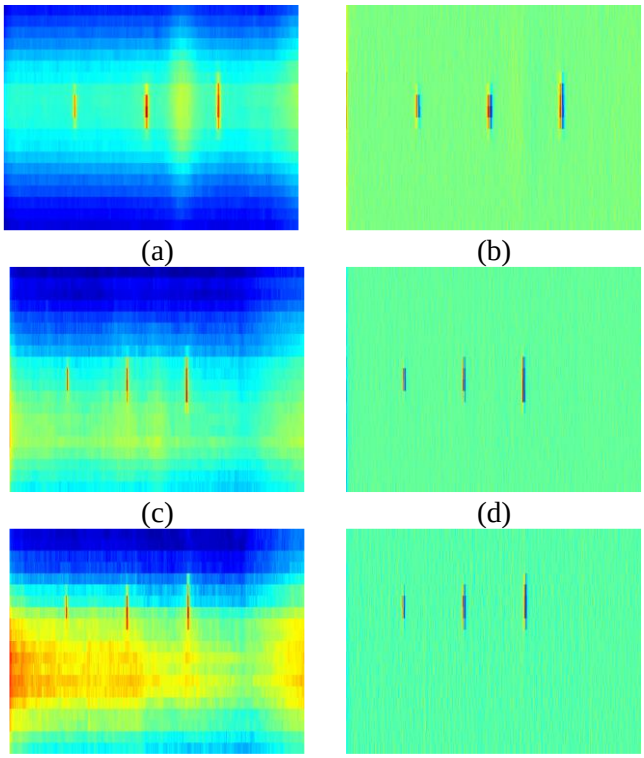

Figure 7 Temperature decay map (TMap) and Derivative map (gradmap)(a)Tmap of N1-N2-N3 (b) gradmap of N1-N2-N3 (c) Tmap N4-N5-N6 (d) gradmap of N4-N5-N6 (e) Tmap of N7-N8-N9 (f) gradmap of N7-N8-N9

4. Conclusion

In this paper, laser scanning thermography for detecting the surface cracks on a titanium sample with EDM notches and oxidation layer is studied. A cobot is used to do laser spot scanning by translating the investigated sample. The peaks from the temperature-time profile provided indications of surface cracks and also the presence of oxidation layer on the surface. The basic heating mechanisms during the laser spot scanning provides insights about the pattern of hotspot generation during the laser scanning. The derivative analysis of the temperature-time profiles was used to differentiate between the crack indication and surface oxide layer indications. The thermal map and the corresponding gradient maps were generated to clearly identify the presence of cracks from the thermal image sequence.

Acknowledgement

This research work was supported by the Agency for Science, Technology and Research (A*STAR) through grants under its Singapore Aerospace Programme Cycle 15 (Grant No. M2115a0093 and M2115a0094) and Polymer Matrix Composites Programme (Grant No. A19C9a0044).

References

[1] X. P. Maldague, *Theory and practice of infrared technology for nondestructive testing*. John Wiley & Sons, 2001.

[2] L. Cartz, *Nondestructive testing*. United States: ASM International, Materials Park, OH (United States), 1995.

[3] T. Li, D. P. Almond, and D. A. S. Rees, "Crack imaging by scanning laser line thermography," *AIP Conf. Proc.*, vol. 1335, no. June 2011, pp. 407–414, 2011, doi: 10.1063/1.3591881.

[4] J. Schlichting, M. Ziegler, C. Maierhofer, and M. Kreutzbruck, "Flying Laser Spot Thermography for the Fast Detection of Surface Breaking Cracks," *18th World Conf. Nondestruct. Test.*, no. April, p. 7, 2012.

[5] P. V Nithin, S. Unnikrishnakurup, C. V Krishnamurthy, M. Zeigler, P. Myrach, and K. Balasubramaniam, "In-line Laser Thermography for Crack Detection: A Numerical Approach," 2015, doi: 10.21611/qirt.2015.0089.

[6] N. Puthiyaveettil, K. R. Thomas, S. Unnikrishnakurup, P. Myrach, M. Ziegler, and K. Balasubramaniam, "Laser line scanning thermography for surface breaking crack detection : modeling and experimental study," *Infrared Phys. Technol.*, vol. 104, no. November 2019, p. 103141, 2020, doi: 10.1016/j.infrared.2019.103141.

[7] S. Beuve, Z. Qin, J. P. Roger, S. Holé, and C. Boué, "Open cracks depth sizing by multi-frequency laser stimulated lock-in thermography combined with image processing," *Sensors Actuators, A Phys.*, vol. 247, pp. 494–503, 2016, doi: 10.1016/j.sna.2016.06.028.

[8] A. Bedoya *et al.*, "Measurement of in-plane thermal diffusivity of solids moving at constant velocity using laser spot infrared thermography," *Meas. J. Int. Meas. Confed.*, vol. 134, pp. 519–526, 2019, doi: 10.1016/j.measurement.2018.11.013.

[9] S. Sfarra, L. Gavérina, C. Pradere, A. Sommier, and J. C. Batsale, "Integration study among flying spot laser thermography and terahertz technique for the inspection of panel paintings," *J. Therm. Anal. Calorim.*, no. 0123456789, 2022, doi: 10.1007/s10973-021-11181-8.

[10] Q. Wang, Z. Zhang, W. Yin, H. Chen, and Y. Liu, "Defect Detection Method for CFRP Based on Line Laser Thermography," *Micromechanics*, vol. 612, no. 13, 2022.

[11] N. Puthiyaveettil, P. Rajagopal, and K. Balasubramaniam, "Influence of absorptivity of the material surface in crack detection using laser spot thermography," *NDT E Int.*, vol. 120, no. December 2020, p. 102438, 2021, doi: 10.1016/j.ndteint.2021.102438.

[12] Philipp Myrach *et al.*, "Thermographic Crack Detection in Hot Steel Surfaces," *19th World Conference on Non-Destructive Testing*, 2016. https://www.researchgate.net/publication/312164547_Thermographic_Crack_Detection_in_Hot_Steel_Surfaces (accessed Sep. 24, 2022).